Mineralogical Magazine, June 1998, Vol. 62(3), pp. 395–407

Parageneses and compositional variations of Sb oxyminerals from Långban-type deposits in Värmland, Sweden

DAN HOLTSTAM

Department of Mineralogy, Swedish Museum of Natural History, Box 50007, SE-104 05 Stockholm, Sweden

PER NYSTEN

Institute of Earth Sciences, Uppsala University, Villavägen 16, SE-752 36 Uppsala, Sweden

AND

KJELL GATEDAL

Xenos Mineral, Rågvägen 7, SE-713 34 Nora, Sweden

ABSTRACT

The Långban, Nordmark and Jakobsberg Mn-Fe deposits contain the only known occurrences of filipstadite and manganostibite (ideal formulae $(Mn, Mg)_2(Sb^{5+}_{0.5}Fe^{3+}_{0.5})O_4$ and $Mn^{2+}_7SbAsO_{12}$, respectively). Filipstadite from Nordmark is newly recognized, and occurs in assemblages with svabite-johnbaumite, calcite, tephroite-forsterite, phlogopite-kinoshitalite, tilasite, ±jacobsite, ±plumbian roméite, ±adelite, ±hedyphane. Manganostibite from Långban and Jakobsberg is reported for the first time, and the mineral is generally associated with katoptrite, tephroite, humite-group minerals, calcite, svabite, allactite, manganosite, hausmannite, jacobsite, spinel *s.s.*, etc. Whereas filipstadite is clearly secondary relative to the major part of the matrix components, manganostibite is believed to have formed coevally with the principal ore and skarn minerals at these deposits.

The previously known compositional ranges are extended. Based on electron-microprobe analyses, Nordmark filipstadite contains 4.1–7.3 MgO, 0.0–0.5 Al_2O_3, 30.5–45.3 MnO, 17.0–40.1 Fe_2O_3, 0.2–0.9 ZnO, 19.9–29.9 Sb_2O_5 (all in wt.%), corresponding to 58–100 mol.% of a pure filipstadite component. Associated jacobsites show Sb_2O_5 contents of up to *c.* 5 wt.%. Manganostibites (all three deposits considered) contain 1.0–2.9 MgO, 2.8–3.8 SiO_2, 57.4–60.3 MnO, 0.2–3.5 Mn_2O_3, 0.3–2.0 Fe_2O_3, 0.0–2.4 ZnO, 21.5–23.0 Sb_2O_5, 7.7–10.0 As_2O_5 (all in wt.%). Si and trivalent cations are incorporated via a $(Mn^{3+},Fe^{3+}) + Si^{4+} = Mn^{2+} + As^{5+}$ exchange mechanism, which improves the local charge-balance at tetrahedral structural sites dominated by As.

KEYWORDS: filipstadite, manganostibite, jacobsite, katoptrite, antimony, Långban, Nordmark, Jakobsberg, Sweden.

Introduction

THE so-called Långban-type localities in south-central Sweden are carbonate-hosted Fe-Mn-(Ba-Pb-As-Sb) deposits (Moore, 1970*a*). They occur within a supracrustal rock sequence dominated by felsic metavolcanics of Svecofennian (~1.9 Ga) age that has been metamorphosed under amphibolite-facies conditions of low-pressure type (Björk, 1986; Lundström, 1995) and to some extent also affected by several intrusive events in the region. From a genetic point of view the deposits are believed to represent metamorphic equivalents of oceanic exhalative-sedimentary deposits (Boström *et al.*, 1979). The Långban mines (lat. 59.86°N, long. 14.27°E) in the Filipstad district, Värmland, are well known for their chemical complexity and mineral species

diversity in skarn and late-vein parageneses (Magnusson, 1930). The Fe (hematite–magnetite) and Mn (braunite–hausmannite) ore bodies occur in close juxtaposition but are chemically well separated from each other, reflecting a presumed order of deposition of the protoliths.

The Nordmark ore field (Nordmarks odalfält; lat. 59.83°N, long. 14.12°E), Filipstad, comprises some twenty small mines and prospects which have mainly been worked for magnetite ore in the past. Subeconomic Mn oxide mineralizations restricted to minor bodies were encountered in the mines Östra Mossgruvan, Kitteln and Brattforsgruvan. The principal constituents of these ore pods were hausmannite, manganosite and secondary pyrochroite, associated with various more or less exotic silicates, arsenates, arsenites and antimonates (Magnusson, 1929). Other minerals, chiefly found dispersed in the carbonate host matrix, are jacobsite, spinel–galaxite solid solutions, periclase, brucite and boron-bearing phases, including blatterite (Raade *et al.*, 1988) and harkerite (Holtstam and Langhof, 1995). The small Jakobsberg mines, situated 1 km SE of Nordmark, were primarily worked for hausmannite ore (Magnusson, 1929).

The purpose of the present paper is to present new paragenetic and mineral-chemical data for two of the principal Sb oxyminerals, filipstadite and manganostibite, found at these deposits, based on observations of recently collected material and museum specimens. The results may give further insights into the conditions of formation of the phases and the crystal-chemical behaviour of the Sb^{5+} cation in a metamorphic environment (cf. Moore, 1970*b*).

Filipstadite

Filipstadite $[(Mn,Mg)_2(Sb^{5+}_{0.5}Fe^{3+}_{0.5})O_4]$ was described as a new, spinel-related mineral from Långban by Dunn *et al.* (1988*a*). Associated phases are jacobsite, calcite and ingersonite. Filipstadite occurs both as isolated, euhedral grains and as overgrowths on (partly replacing) jacobsite. From the composition and crystal symmetry (orthorhombic and pseudocubic, with an edge length of 8.640(1) Å for the cubic subcell) the mineral was deduced to possess a modified spinel structure, resulting from the ordering of Sb^{5+} and Fe^{3+} over two different (octahedral) crystallographic sites. The crystal chemistry of this mineral has, however, not been studied in detail.

A second occurrence at Jakobsberg was reported by Holtstam (1993); this filipstadite coexists with hausmannite, calcite, forsterite, phlogopite and other minerals. The present work is the first record of the mineral at Nordmark, where it is not uncommon as judged from the results of our field collecting activities.

Manganostibite

Igelström (1884) described manganostibite as a new Mn-Sb-As oxide mineral from the mine Östra Mossgruvan at Nordmark, where it was found as scattered grains in hausmannite-bearing carbonate rock. Moore (1968) discussed the crystal chemistry of the mineral, and later formulated its ideal composition as $Mn^{2+}_7AsSbO_{12}$. A detailed crystal structure analysis (Moore, 1970*b*) showed manganostibite to be orthorhombic, space group *Ibmm*, with a = 8.727(5), b = 18.847(6), c = 6.062(4) Å and Z = 4. The structure is based on cubic close-packed layers of O atoms parallel to {130}; Sb and As occupy octahedral and tetrahedral interstices, respectively, whereas Mn is distributed over three six-coordinated sites (denoted *M*1, *M*2, and *M*3) and one four-coordinated site (*T*). Dunn (1986) presented some new chemical data for manganostibite, and drew attention to the fact that it usually contains significant Si and possibly some Mn^{3+}. In this study we present more data from Nordmark; in addition two further occurrences of the mineral, at Långban and Jakobsberg, are reported.

Methods of investigation

Polished rock sections were studied under the polarizing microscope and the scanning electron microscope. Powder X-ray diffraction (PXRD) and energy-dispersive X-ray (EDS) microanalysis were used as an aid in mineral identification. Electron microprobe (EMP) analysis was also employed. The Sb-containing phases and some associated minerals have been analysed quantitatively with a Cameca SX50 instrument, operated at 20 kV and 12 nA, and using natural and synthetic standards: vanadinite (Pb-*M*β), baryte (Ba-*L*α), stibnite (Sb-*L*α), GaAs (As-*L*α), $MnTiO_3$ (Mn,Ti-*K*α), Fe_2O_3 (Fe-*K*α), ZnS (Zn-*K*α), MgO (Mg-*K*α), Al_2O_3 (Al-*K*α), wollastonite (Ca-*K*α), orthoclase (K-*K*α) and albite (Na, Si-*K*α). Data reduction was made using a Cameca version of the PAP (Pouchou and Pichoir, 1984) routine.

TABLE 1. Mineral assemblages

Sample no.	cal	flp	hed	jac	hau	ktp	mic	msb	ol	rom	sva	til	others
950228 N	×	×	(×)				×		×	(×)	×		adelite, lead, stibarsen
950229 N	×	×	×	×					×	×	×	×	
960274 N	×	×	(×)	×			×		×		×	×	baryte
970001 N	×	×	(×)	×			×			×			allactite, lead
496/1 N	×	×		×	×			×			×		adelite, sonolite, spinel
KG1 N	×				×			×			×	×	allactite?, baryte
KG2 N	×	×			×			×		×	×	×	pyrochroite
KG3 N	×			×		×		×			×	×	
KG4 J	×			×	×	×		×	×		×		allactite, copper
KG5 J	×					×	(×)	×	×				manganhumite?
KG6 L	×				×			×	×				manganosite, pyrochroite
PN1 N	×							×					manganosite, pyrochroite

Abbreviations: cal = calcite, flp = filipstadite, hau = hausmannite, hed = hedyphane, jac = jacobsite, ktp = katoptrite, mic = mica, msb = manganostibite, ol = olivine, rom = roméite, sva = svabite-johnbaumite-turneaureite, til = tilasite. (×) = the mineral constitutes less than 2% of the sample volume.
N, J and L refer to samples from Nordmark, Jakobsberg and Långban, respectively.

Description of the filipstadite-bearing samples

The Nordmark filipstadite occurs in fine-grained, granular arsenate-oxide-silicate rock samples, four of which were collected from the dumps of the mine Kitteln by one of us (KG), and which now are in the collections of the Swedish Museum of Natural History (catalogue Nos are indicated in Table 1). Two additional samples, #496/1 and #KG2 from the Mineralogical Museum of Uppsala University, are described below as manganostibite specimens. The mineral assemblages have been summarized in Table 1. The chemical formulae of some unusual species discussed are listed in Table 2.

The dominant arsenate species is svabite-johnbaumite. Tilasite or adelite are also important constituents. These arsenates often occur in close association with each other, and appear as irregularly shaped, anhedral to subhedral grains with sizes typically ranging from 0.2 to 0.4 mm. The fluorine analyses of the phases produced only semi-quantitative results, indicating variable F contents or variable analytical quality, or both; the members of the svabite-johnbaumite series will thus simply be referred to as svabite in this paper. Svabite also contains significant Cl (estimations from EDS analyses suggest substitutions corresponding up to *c.* 25% of a turneaureite component) and minor Pb, Mn and P. It is characterized by an intense orange-yellow fluorescence under 254 nm UV light. Tilasite is close to the ideal composition with respect to the cation contents, whereas adelite has significant Mn proxying for Mg [atomic Mn/(Mn + Mg) = 0.17]. Hedyphane is a subordinate phase in these samples, mostly found as irregular blebs included in the major arsenates. In sample #970001 hedyphane appears as relicts, and has largely been replaced by a phase whose composition lies close to a magnesian allactite [$(Mn_{6.24}Mg_{0.67}Ca_{0.09})$

TABLE 2. End-member compositions of some mineral species mentioned in the text

adelite	$CaMg(AsO_4)(OH)$
bindheimite	$Pb_2Sb_2O_6(O,OH)$
hedyphane	$Pb_3Ca_2(AsO_4)_3Cl$
ingersonite	$Ca_3MnSb_4O_{14}$
johnbaumite	$Ca_5(AsO_4)_3(OH)$
katoptrite	$Mn_{13}Al_4Sb_2Si_2O_{28}$
långbanite	$Mn^{2+}_4Mn^{3+}_9SbSi_2O_{24}$
melanostibite	Mn_2SbFeO_6
nadorite	$PbSbO_2Cl$
parwelite	$Mn_5SbAsSiO_{12}$
roméite	$Ca_2Sb_2O_6(O,OH)$
svabite	$Ca_5(AsO_4)_3F$
tilasite	$CaMg(AsO_4)F$
turneaureite	$Ca_5(AsO_4)_3Cl$

$(AsO_4)_2(OH)_8$]; the Pb which has been released in the process occurs as the native metal in formless grains. Minute, spongy grains of a mimetite-like phase also occur in this sample, as well as cerussite. Hedyphane in #950229 is barian, with Ba/(Ba + Pb) = 0.15.

The silicates encountered are mica (phlogopite-kinoshitalite) and olivine (forsterite-tephroite). The mica shows significant intrasample compositional variations in terms of K/Ba and Al/Si ratios (Table 3); in #960274 some crystals were found to have a phlogopite core rimmed by kinoshitalite. Olivine compositions range from $Fo_{61}Te_{39}$ to $Fo_{30}Te_{70}$.

Manganoan calcite, with Mn/(Mn + Ca) $\simeq$ 0.10, is common in all samples; calcite as a late crack-filling in #950229 is distinctly lower in Mn, with the ratio 0.04. A few anhedral grains of Pb-bearing stibarsen, up to 80 μm in their greatest dimension, were found with filipstadite, calcite and minute blebs of native lead in #950228; the composition as determined with EMP analysis of two grains is $Sb_{1.00}As_{0.93}Pb_{0.07}$.

The oxide fraction is usually concentrated in diffuse bands or patches of up to a few mm wide. In #950228 filipstadite occurs as equant, euhedral to subhedral grains, typically with a hollow outline and 'atoll' texture (Fig. 1A). Specimen #950229 carries aggregates of adjoining subhedral grains consisting of jacobsite mantled by filipstadite (Fig. 1B). The sample is also rich in plumbian roméite, which occurs as equant, mostly euhedral grains (20–100 μm across), in stripes along with the portions carrying filipstadite-jacobsite; an average composition based on four EMP analyses is $Na_{0.10}Ca_{1.25}Pb_{0.26}Mn_{0.12}Sb_{1.73}Fe_{0.27}O_6(O,OH,F)$. In #960274 jacobsite occurs as single grains overgrown by filipstadite,

TABLE 3. Microprobe analyses of mica and olivine

	#950228 mic grain #1	#950228 mic grain #2	#960274 mic core	#960274 mic rim	#950229 ol	#960274 ol
SiO_2	29.33	27.46	31.11	25.40	35.29	31.44
Al_2O_3	17.67	17.83	18.31	19.01	0.01	0.01
Fe_2O_3	0.36	0.40	0.94	0.96	–	–
FeO	–	0.–	–	–	0.49	0.28
MnO	1.95	2.05	3.18	2.79	33.50	53.73
MgO	22.76	22.09	21.64	20.13	29.80	13.43
CaO	0.00	0.00	0.00	0.05	0.22	0.18
BaO	13.63	19.25	12.80	23.12	0.00	0.00
Na_2O	0.02	0.06	0.00	0.00	0.00	0.00
K_2O	5.72	3.69	5.95	2.21	0.00	0.00
Total	91.44	92.83	93.93	93.67	99.31	99.07
Formula proportions						
Si	2.38	2.29	2.47	2.19	0.97	0.97
Al	1.69	1.76	1.71	1.93	0.00	0.00
Fe^{3+}	0.02	0.03	0.06	0.06	–	–
Fe^{2+}	–	–	–	–	0.01	0.01
Mn	0.14	0.15	0.21	0.20	0.78	1.40
Mg	2.75	2.75	2.55	2.59	1.23	0.61
Ca	0.00	0.00	0.00	0.00	0.01	0.01
Ba	0.43	0.63	0.40	0.78	0.00	0.00
Na	0.00	0.00	0.00	0.00	0.00	0.00
K	0.59	0.39	0.60	0.25	0.00	0.00
Σ cations	8.00	8.00	8.00	8.00	3.00	3.00
O_{calc}	10.94	10.98	11.05	11.06	3.98	3.97

and as almost skeletal inclusions in larger filipstadite aggregates (Fig. 1C). Sample #970001 contains euhedral to subhedral filipstadite enclosing formless jacobsite cores.

Description of the manganostibite-bearing samples

Nordmark samples

A clear spatial connection between Mn arsenates (e.g. allactite) and manganostibite is evident at Nordmark (*Kitteln*), where the latter mineral is especially concentrated in calcite-and svabite-rich matrices close to allactite-bearing fissures. Manganostibite forms anhedral slightly elongated crystals coexisting with iron-bearing hausmannite (5.8 wt.% Fe_2O_3), baryte and tilasite/adelite (#KG1). It is also common as inclusions within hausmannite in the carbonate host rock. A relatively wide, straight veinlet carrying euhedral allactite(?) as well as thinner, anastomosing fissures preferentially cut the hausmannite.

Manganostibite also occurs as several mm large, irregular crystals which contain small rounded inclusions of calcite, hausmannite and a chemically complex spinel-structure phase. The latter is weakly but distinctly anisotropic and with a composition of $Mn_{1.00}Mg_{0.21}Fe^{3+}_{0.84}Mn^{3+}_{0.76}Al_{0.08}Sb_{0.11}O_4$ it lies close to iwakiite, a tetragonal $Mn(Fe^{3+},Mn^{3+})_2O_4$ phase (Matsubara *et al.*, 1979). Some of these grains contain minute cores of a phase with a lower reflectance, shown to be filipstadite (cf. below). Narrow zones surrounding these cores exhibit a characteristic breakdown texture, with lamellar parting planes oriented in two different directions; the appearance is similar to 'vredenburgite' described from the Fe-Mn-O system (Mason, 1943). The oxide phases plus minor tilasite occur reasonably concentrated in bands enclosed by the calcite+svabite matrix. Pyrochroite is occasionally present as a thin film along grain boundaries of calcite.

The largest concentration of manganostibite is seen in sample #KG3, where the mineral coexists with katoptrite, tilasite and Sb-bearing jacobsite in a matrix of calcite and svabite-johnbaumite (Fig. 2). Very small, whitish grains with a high reflectance have been noted as an accessory phase; they are tentatively identified as stibarsen. Katoptrite is found as euhedral crystals in subparallel bands, displaying the typical cleavage and slightly lower reflectance of this phase as compared to manganostibite. This type of katoptrite often shows poikiloblastic inclusions of carbonate, and the crystal size is distinctly smaller than that of manganostibite, which may reach several mm. Chemical analyses of katoptrites are given in Table 4.

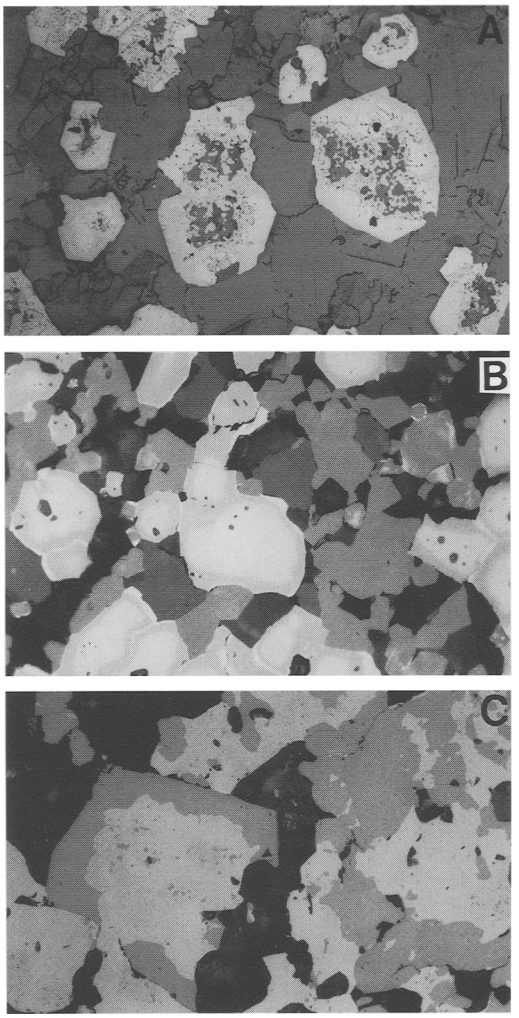

FIG. 1. Photomicrographs (reflected polarized light) of filipstadite-bearing assemblages. (A) Hollow filipstadite grains in a mica-calcite matrix (#950228). (B) Jacobsite (white) mantled by thin filipstadite rims, with roméite (grey) and calcite (#950229). (C) Intergrown filipstadite (dark grey) and jacobsite (light grey) with arsenates (#960274). Fields of view are 0.2 × 0.3 mm.

Manganosite ore has been found to carry local concentrations of either katoptrite or manganostibite. The latter mineral is seen in sample #PN1, where it occurs as rounded to angular inclusions

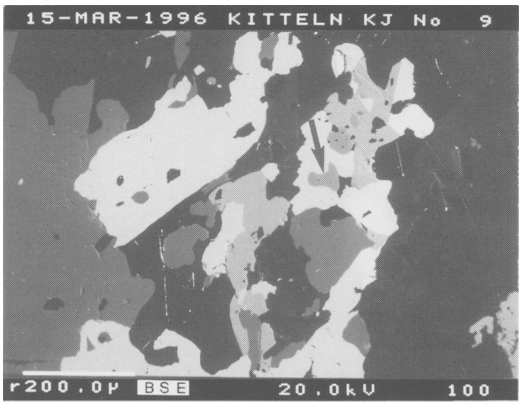

FIG. 2. Backscattered-electron image of manganostibite (white) in specimen #KG3, contiguous to katoptrite (light grey), tilasite (dark grey) and calcite (black). The arrow points to an intermediary grey phase, which is jacobsite. Scale bar (lower left corner) equals 200 µm.

($\leqslant$1 mm) in manganosite [$(Mn_{0.98}Mg_{0.02})O$] grains and in the carbonate host. Manganostibite displays a somewhat lower reflectance and similar hardness as compared to manganosite, but it is easily detected by the strong anisotropy, displaying brownish to violet tints when the polarizers are slightly uncrossed. A coexisting spinel phase exhibits an unusual composition $(Mn^{2+}_{0.86}Mg_{0.12}Zn_{0.02})(Fe^{3+}_{0.83}Mn^{3+}_{0.80}Mn^{2+}_{0.02}Al_{0.31}Ti_{0.02}Sb^{5+}_{0.02})O_4$. Pyrochroite occurs rimming euhedral manganosite and as late fracture-fillings. At least two chemically different Mn-silicates are also present; one composition points towards a magnesian leucophoenicite or manganhumite [Mn/(Mn + Mg + Ca) = 0.58; Me^{2+}/Si = 2.36], the other composition suggests alleghanyite [Mn/(Mn + Mg + Ca) = 0.56; Me^{2+}/Si = 2.57].

Macroscopically, sample #496/1 is an even-grained carbonate rock with more or less densely spaced bands of hausmannite and jacobsite. A silicate phase corresponding to a magnesian sonolite as determined from PXRD patterns is also abundant, whereas small pods of a yellow adelite are less common. Irregular bands with anhedral grains of a svabite-type arsenate cut the sample; EDS analysis of this phase shows high concentrations of Cl, corresponding to *c.* 70% of the turneaureite component. The investigation by microscope reveals fairly abundant, slightly elongated manganostibite grains of <1 mm in size. Subhedral jacobsite grains often occur as inclusions, whereas minor filipstadite has been noted on the contact between subgrains of manganostibite. Small (100–200 µm), euhedral laths of a pinakiolite-like mineral have also been found. These phases are dispersed in a calcite marble matrix. Occasional, euhedral crystals ($\leqslant$300 µm) of yellowish manganoan zincian spinel *sensu stricto*, with square cross-sections, may also be noted.

TABLE 4. Microprobe analyses of katoptrite

	#KG3 *n* = 1	#KG5 *n* = 2
MgO	2.36	1.82
Al_2O_3	10.45	9.85
SiO_2	7.57	8.15
CaO	n.d.	0.06
MnO	53.84	55.11
Fe_2O_3	2.79	2.05
ZnO	0.49	1.29
Sb_2O_5	22.09	21.23
As_2O_5	0.38	0.17
Total	99.97	99.73
Formula proportions based on 21 cations		
Mg	0.92	0.71
Al	3.24	3.06
Si	1.99	2.15
Ca	–	0.02
Mn^{2+}	11.99	12.30
Fe^{3+}	0.55	0.41
Zn	0.10	0.25
Sb^{5+}	2.16	2.08
As^{5+}	0.05	0.02
O_{calc}	28.20	28.04

n = number of point analyses. n.d. = not detected

Jakobsberg samples

At Jakobsberg, manganostibite seems to be less frequent. In #KG4 it forms aggregates of subhedral, skeletal crystals up to 200 µm long in a banded matrix of allactite [$(Mn_{6.72}Ca_{0.14}Mg_{0.06}Zn_{0.04})(AsO_4)_2(OH)_8$], calcite and euhedral katoptrite crystals. Small, rounded jacobsite grains occur in a svabite matrix appearing in other portions of the sample. Hausmannite of composition $(Mn^{2+}_{0.97}Zn_{0.03})(Mn^{3+}_{1.82}Fe_{0.14}Al_{0.04})O_4$ is the dominating oxide present in this sample as well as

in #KG5, where manganostibite also coexists with native copper and tephroite ($Fo_{13}Te_{87}$).

Långban sample

Sample #KG6, which originates from the 130 m level of the Norrbotten working at Långban, mainly consists of hausmannite-impregnated calcite. However, the most conspicuous mineral present is bright green manganosite, surrounded by a thin rim of pyrochroite. The latter mineral also forms subparallel, thin fissure-fillings which cut all other phases. Anhedral crystals of tephroite ($Fo_{41}Te_{59}$) are also common in the carbonate matrix. Native copper has been noted as an accessory phase.

Manganostibite, which has not been reported earlier from this deposit, is a fairly rare phase in the association. It forms small ($\leqslant 30$ μm), anhedral crystals intergrown with the olivine and displays a strong anisotropy in brown to violet colours. This behaviour, together with reddish-brown internal reflections, is diagnostic for the mineral.

Filipstadite mineral chemistry

Representative analyses of the spinel-type oxides (filipstadite and jacobsite) are given in Table 5. They reveal a wide compositional spectrum for filipstadite, compared with earlier data. The Sb-bearing jacobsite is, to the best of our knowledge, also something new. The atomic proportions in Table 5 were calculated on the basis of three cations per formula unit (pfu). Assuming that these spinels are stoichiometric, with four O atoms pfu, only moderate amounts of Mn^{3+} or Fe^{2+} would mostly be required to charge-balance the formulae. For filipstadite, up to 5% of total Mn should be recalculated to the trivalent state. An exception is #KG2, where $Mn^{3+}/(Mn^{3+} + Mn^{2+}) = 0.17$ for filipstadite. This could be compared with the filipstadite from Jakobsberg [$(Mn^{3+}/(Mn^{3+} + Mn^{2+}) = 0.22$] coexisting with hausmannite (Holtstam, 1993).

The Nordmark filipstadite is low in Mg, with $X_{Mg} = Mg/(Mg + Mn^{2+}) = 0.14-0.25$, compared to $X_{Mg} = 0.37$ for the type material (Dunn *et al.*, 1988*a*). Occasionally ZnO may reach a concentration of 0.8 wt.%, which is still a lower value than found for the Jakobsberg material (1.9–2.1 wt.%; Holtstam, 1993). TiO_2 is present in trace amounts only, and often close to the detection limit ($\leqslant 0.05$ wt.%). Antimony contents range from close to the ideal value of 0.5 atoms pfu in #950228 to 0.3 atoms pfu in #950229. This decrease is strongly correlated with a decrease in the number of divalent cations (2.1–1.5 atoms pfu), and an increase in Fe (0.5–1.2 atoms pfu). Obviously, there is a relation to a charge-coupled substitution mechanism of the type $3Fe^{3+} = 2(Mn, Mg)^{2+} + Sb^{5+}$. This kind of cation exchange is rarely encountered in the mineral kingdom, but the expression was recently invoked to explain the incorporation of Sb^{5+} in magnetoplumbite (ideally $PbFe_{12}O_{19}$) from Långban-type deposits (Holtstam, 1994).

In other words, the filipstadites investigated contain up to *c.* 40 mol.% of a $(Mn,Mg)Fe_2O_4$ (jacobsite-magnesioferrite) spinel in solid solution, plus minor $MnMn_2O_4$ or $FeFe_2O_4$ components. To exceed the ideal Sb contents of 0.5 atoms pfu in filipstadite, incorporation of a monovalent cation of suitable size (which is absent in the present paragenesis) or the presence of cation vacancies would be required. The purported cation ordering in filipstadite, and the deviation from cubic crystal symmetry, prohibits a complete solid solution series with jacobsite. The latter mineral, as estimated from the present data, contains up to 12 mol.% of the $(Mn,Mg)_2(Sb_{0.5}Fe_{0.5})O_4$ component. The compositional gap may, however, be even smaller; for sample #950229, where there are diffuse reaction contacts between the two spinel-like phases, the spatial resolution of the EMP does not allow reliable concentration values to be determined. Compare the PXRD pattern of the oxide fraction in #960274 (Fig. 3A), which shows well separated 511 and 440 peaks for filipstadite and jacobsite, with the recording for #950229 (Fig. 3B). Here the two pairs are not resolved; this fact is consistent with a topotactic intergrowth between Sb-poor filipstadite and Sb-rich jacobsite having similar values for the cubic (sub)cell parameter. Furthermore, a #970001 grain was found to contain irregular patches ($\leqslant 20$ μm) with Sb_2O_5 contents around 8 wt.% (equivalent to *c.* 23 mol% of the filipstadite component). These spots may, however, represent a metastable phase or constitute suboptical intergrowths of jacobsite-filipstadite.

Some grains in #950228 are irregularly zoned and certain sectors are compositionally distinct by their high Si contents. Figure 4 shows rim-to-core element profiles based on EMP point analyses of a heterogeneous grain. They clearly show positive correlations between the Mn, Sb, Mg and Si contents; these elements are in turn antipathetical *vs.* Fe. The most drastic changes are in the Fe_2O_3

TABLE 5. Selected spinel-type oxide analyses

	flp #496/1 $n = 1$	flp #KG2 $n = 2$	flp #950228A $n = 1$*	flp #950228A $n = 1$*	flp #960274A $n = 5$	flp #960274B $n = 8$	flp #970001 $n = 2$	flp #950229 $n = 6$	jac #960274A $n = 12$	jac #960274B $n = 7$	jac #950229 $n = 4$	jac #970001 n = 2
MgO	6.82	6.35	7.73	6.40	4.22	4.12	7.26	6.55	1.74	1.57	2.72	2.28
Al_2O_3	0.32	0.31	0.30	0.42	0.48	0.29	0.26	0.04	2.35	1.81	0.13	1.22
SiO_2	0.04	0.12	2.11	0.09	0.00	0.00	0.00	0.00	0.00	0.00	0.00	0.00
TiO_2	0.13	0.00	0.00	0.10	0.07	0.02	0.00	0.00	0.16	0.16	0.01	0.05
MnO	41.43	48.91	49.62	45.32	41.52	42.59	30.49	33.30	34.48	33.25	29.06	31.70
Fe_2O_3	20.92	16.84	5.60	17.00	31.93	27.51	37.49	40.14	57.31	58.93	63.77	62.16
ZnO	0.63	0.00	0.46	0.46	0.21	0.16	0.21	0.88	0.24	0.34	0.81	0.12
Sb_2O_5	29.41	25.90	33.91	29.90	22.29	25.14	24.02	19.92	3.54	3.58	4.39	1.73
Total	99.70	98.43	99.73	99.69	100.72	99.83	99.73	100.83	99.82	99.64	100.89	99.26
Formula proportions												
Mg	0.42	0.38	0.47	0.39	0.25	0.25	0.43	0.38	0.10	0.09	0.15	0.13
Al	0.02	0.02	0.02	0.02	0.02	0.01	0.01	0.00	0.10	0.08	0.01	0.05
Si	0.00	0.00	0.09	0.00	0.00	0.00	0.00	0.00	0.00	0.00	0.00	0.00
Ti	0.00	0.00	0.00	0.00	0.00	0.00	0.00	0.00	0.00	0.00	0.00	0.00
Mn^{2+}	1.44	1.69	1.72	1.59	1.42	1.49	1.27	1.11	1.11	1.08	0.94	1.02
Fe^{3+}	0.65	0.52	0.17	0.53	0.97	0.86	0.92	1.19	1.63	1.69	1.82	1.77
Zn	0.02	0.00	0.01	0.01	0.01	0.00	0.01	0.03	0.01	0.01	0.02	0.00
Sb^{5+}	0.45	0.39	0.52	0.46	0.33	0.39	0.36	0.29	0.05	0.05	0.06	0.03
Σ cations	3.00	3.00	3.00	3.00	3.00	3.00	3.00	3.00	3.00	3.00	3.00	3.00
Charge (+)	8.02	7.72	7.91	7.93	7.98	8.04	8.00	8.06	7.88	7.92	8.01	7.91

n = number of point analyses. A and B refer to different portions of a petrographic section.
* analysis of a point with extreme composition, on a heterogeneous grain.

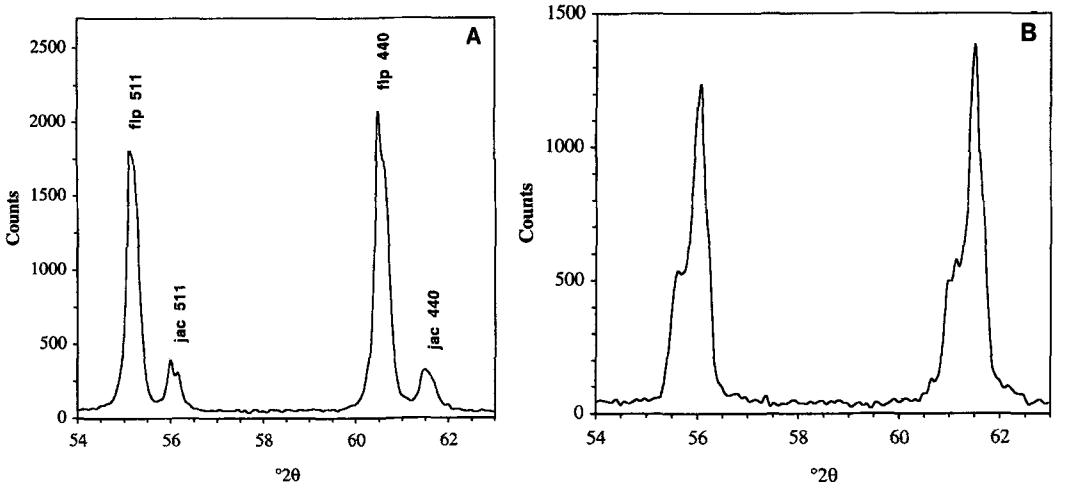

FIG. 3. Powder diffraction patterns (Cu-$K\alpha$ X-ray radiation) of the spinel-related oxide fractions in #960274 (A) and #950229 (B).

and SiO_2 concentrations, ranging from 5.6 to 17.0 wt.% (0.17–0.53 atoms pfu) and 0.1 to 2.2 wt.% (0.0–0.09 atoms pfu), respectively. A visible zoning in the reflectance of the grain is clearly related to this variation, with the brighter parts having the highest Fe and lowest Si contents.

The straight line in the plot of Fig. 5 shows the correlation between Fe and Sb in this sample for the Fe-rich parts; the relation is explained by the coupled Fe^{3+}-Sb^{5+} replacement discussed above. Apparently the Fe contents could then be decreased further, far below 0.5 atoms pfu. At this stage, however, the filipstadite is saturated with respect to Sb^{5+}. The Fe-Si variations (Fig. 6) shows a similar break in the trend and reveals a gap between points with little Si and those with

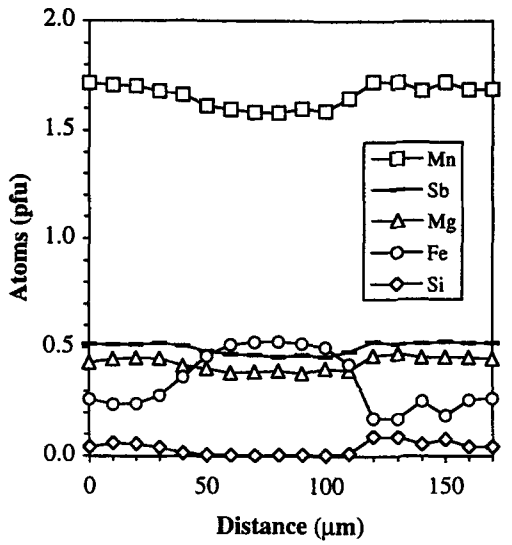

FIG. 4. Step scanning profile from rim (left) to core (right) of a heterogeneous grain in #950228.

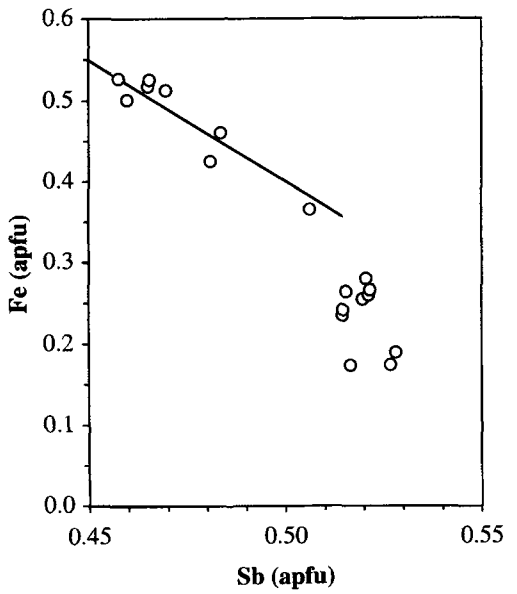

FIG. 5. Plot of Fe *vs.* Sb for sample #950228. The slope of the auxiliary line is −3.

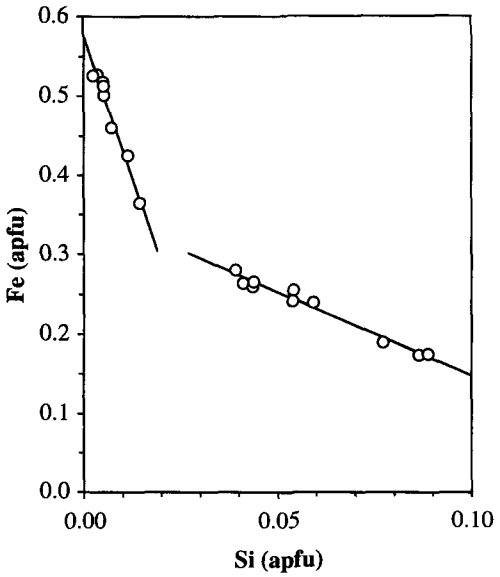

FIG. 6. Fe-Si variations in #950228. The straight lines merely serve as a guide for the eye.

higher contents. The latter can be fitted with a regression line ($R^2 = 0.97$), for which the slope is close to -2. It is suggested that the phase is depleted in iron by a $(Mn, Mg)^{2+} + Si^{4+} = 2\ Fe^{3+}$ substitution, likely to occur for bulk compositions with high Sb/Fe ratios.

The present data thus suggest that we are dealing with a new, discrete phase intimately intergrown with filipstadite, in the portions with lowest reflectance. In fact, this material is optically and compositionally rather similar to the 'phase X' of Holtstam (1993), which was interpreted as a replacement product of the Jakobsberg filipstadite. It is noteworthy that Fe-rich oxide (e.g. jacobsite) is absent in both assemblages. The PXRD data for the oxide fraction of the Nordmark #950229 sample suggest that the new phase also possesses a spinel-type structure as the pattern is quite similar to that of pure filipstadite, but with additional, weaker lines. The structural role of Si is of course uncertain; until the phase can be be isolated and made available for detailed X-ray investigations, we can only speculate about this. The well known preference of Si^{4+} for low coordination geometries makes it likely that it enters tetrahedral sites of the spinel-type structure. Ordering of the cation over a fraction of these positions is a possible cause of the superstructure formation.

Manganostibite mineral chemistry

In Table 6, representative analyses of manganostibite are given. For #KG1 a traverse of closely spaced point analyses was collected along a 0.3 mm crystal and the results indicated a uniform composition. The structural formulae have been normalized on the basis of nine cations and a fraction of Mn present has been computed as Mn^{3+} to balance twelve O atoms. The Jakobsberg sample (#KG4) is distinguished by its high ZnO and low MgO concentrations. The more interesting variations, however, are related to the high-charged cations. The As/Si ratios range from 2:1, the same value as reported for the material examined by Dunn (1986), to near 1:1. This variation is possible through the exchange mechanism $Mn^{3+} + Si^{4+} = Mn^{2+} + As^{5+}$; as seen from the Nordmark #496/1 sample, the presence of Fe^{3+} can also be of importance.

All modern chemical data show substantial amounts of Si to be present in manganostibite. In fact, the present samples approach the hypothetical 'end-member' compound $(Mn^{2+}_{6.5}Mn^{3+}_{0.5})Sb(As_{0.5}Si_{0.5})O_{12}$, and it is suggested that Si and Mn^{3+} or Fe^{3+} play a crucial role in stabilizing the mineral. An inspection of the electrostatic bond valences tabulated by Moore (1970*b*) for 'ideal' manganostibite provides the simplest explanation for this: two considerably oversaturated oxygen atoms appear as ligands to the tetrahedrally coordinated As atom. Replacement by some Si^{4+}, which has an ionic radius comparable to that of As^{5+} (Shannon, 1976), will contribute to improving the local charge balance and hence an increased structural stability. We furthermore assume that the trivalent atoms are ordered at the *M*1 site, which is the smallest in terms of metal-O bond distances, and also possesses a tetragonal distortion (elongation) favourable for incorporation of a Jahn-Teller species like Mn^{3+} (Moore, 1970*b*). It is also noticeable that the present samples contain Sb in excess of one atom pfu. The surplus is in most cases too large to be ascribed to analytical error alone; we therefore suspect that a fraction of the Sb contents is present at *M*1 as well.

Concluding discussion

The Sb oxyminerals discussed have locally been found to be more common in the Långban-type deposits than assumed previously; on the other hand, these localities remain the only known

TABLE 6. Microprobe analyses of manganostibite

	#KG1 $n = 42$	#KG3 $n = 2$	#KG4 $n = 4$	#KG6 $n = 3$	#PN1 $n = 2$	#496/1 $n = 1$
MgO	2.14	1.37	0.99	1.79	2.87	2.52
CaO	n.d.	n.d.	0.09	n.d.	n.d.	n.d.
MnO	59.78	60.33	58.36	60.26	57.37	58.33
Mn_2O_3	2.05	1.89	3.48	2.50	2.64	0.22
Fe_2O_3	0.50	0.90	0.48	0.31	0.65	1.96
ZnO	0.32	0.62	2.35	n.d.	0.97	1.34
Sb_2O_5	22.66	22.87	22.62	23.00	21.93	22.51
As_2O_5	9.71	9.19	7.69	8.92	10.04	10.03
SiO_2	2.90	3.02	3.85	3.26	2.79	2.82
Total	100.06	100.19	99.91	100.04	99.26	99.73
Formula proportions based on 9 cations and 12 oxygens						
Mg	0.40	0.26	0.18	0.33	0.53	0.47
Ca	–	–	0.01	–	–	
Mn^{2+}	6.30	6.38	6.17	6.35	6.05	6.16
Mn^{3+}	0.20	0.18	0.33	0.24	0.25	0.02
Fe^{3+}	0.04	0.09	0.05	0.03	0.06	0.18
Zn	0.02	0.06	0.22	–	0.09	0.12
Sb	1.05	1.06	1.05	1.06	1.01	1.04
As	0.63	0.60	0.50	0.58	0.66	0.65
Si	0.36	0.37	0.48	0.41	0.35	0.35
^{iv}(As+Si)	0.99	0.97	0.98	0.99	1.01	1.00

n = number of point analyses. n.d. = not detected

occurrences world-wide. An obvious conclusion is that favourable geological conditions for the formation of these phases are exceedingly rare. It is, above all, controlled by bulk rock compositions (high Mn, As and Sb contents). Low a_{H_2S} must also be critical (to prevent sulfidation of As and Sb) and high f_{O_2} values (probably above the Fe_2O_3-Fe_3O_4 buffer) are necessary.

An important question is when Sb was introduced to the system. Was the element contained within the volcano-sedimentary precursor, or has it invaded at a later stage? Available information supports the former suggestion. As far as Långban is concerned, Magnusson (1930) came to this conclusion as major concentrations of the element occur in various constituents of typical early reaction skarns contemporaneous with the ore formation. Manganostibite, katoptrite, roméite and Sb-bearing jacobsite also belong to this generation. For example, in our study, manganostibite was found as inclusions in manganosite, a mineral which is believed to have formed under peak-metamorphic conditions (via decomposition of Mn carbonate). Our opinion, therefore, is that Sb precipitated from volcanic exhalations, along with Mn, Pb, Ba and As, into a progenitor of yet unknown nature. We are thus dealing with an essentially isochemical system, but reworking during metamorphism, deformation and one or more stages of hydrothermal activity is anticipated. The mobility of Sb^{5+} is high under oxidizing conditions, as expected from extrapolation of room-temperature thermodynamic data (Wink, 1996).

There are relatively few Sb-containing phases known in the system CaO-MgO-Al_2O_3-SiO_2-MnO-Mn_2O_3-Fe_2O_3-As_2O_5-Sb_2O_5. If a hydrous component is added to it, the diversity will undoubtedly increase, but mainly with typical weathering products. Parwelite is relatively close to manganostibite in composition, but was not found in the present rocks. Melanostibite belongs to the ilmenite structure type and is only known

from the mine Sjögruvan, a small Långban-type deposit situated in Hällefors district, Örebro (Moore, 1968). The lack of these phases in our material is presumably explained by the bulk rock chemistry (the Mn/Sb ratios in essence); only for systems with very high Sb contents should we expect to find these minerals. Ingersonite has a crystal structure derived from that of pyrochlore, and is chemically akin to roméite, another pyrochlore-related compound. Ingersonite is, however, restricted to a very Sb-rich Långban paragenesis (Dunn *et al.*, 1988*b*), and probably requires a higher Sb_2O_5-activity to crystallize. It is also possible that the presence of Pb^{2+} in the assemblages is favourable for the stabilization of roméite (i.e. a roméite-bindheimite solid solution). Långbanite is quite abundant in some Långban-type skarns, but it probably requires higher f_{O_2} levels than katoptrite to form; it contains essential Mn^{3+} and is frequently found to coexist with braunite (e.g. Nysten and Ericsson, 1994). Note that we have excluded Sb^{3+} from the present discussion. Most of the Sb-containing minerals mentioned are structurally well characterized (filipstadite is an exception), and the data are in favour of Sb^{5+}. Recent detailed crystal-chemical analyses of oxyminerals from metamorphosed Mn-deposits agree that the pentavalent form of antimony is more or less sole prevailing (Brugger *et al.*, 1997; Smith and Perseil, 1997). In the Långban-type deposits, Sb^{3+} seems to be confined to the polymorphs of Sb_2O_3 and the oxyhalide nadorite, all of them appearing in late-vein parageneses only (Moore, 1970*a*).

The textural observations are consistent with the idea that filipstadite has grown on pre-existing jacobsite (when present), and partly replaced that mineral. In the absence of a spinel nucleus, the mineral has instead precipitated along grain boundaries of other phases and the characteristic atoll texture developed. In these situations, where Fe/Sb ratios are intrinsically low, the unnamed, spinel-related Sb-oxide (with significant Si) will frequently also form. The Mn^{3+} can obviously replace Fe^{3+} to some extent in filipstadite, *vide supra*, but Jahn-Teller distortion is expected to put a constraint on this kind of substitution. In conclusion, the 'filipstaditization' is a relatively late process that is related to Sb remobilization (possibly preceeded by roméite breakdown); this might be connected to the development of fissure systems in the Långban-type deposits, yet at conditions different from those responsible for the formation of reduced phases (like native lead and Pb-bearing stibarsen). An exception from the general mechanism of formation is seen in sample #KG2, where filipstadite appears as cores in an Mn^{3+}-rich, Sb-bearing spinel phase. In this case the central part of the spinel host has evidently decomposed, exsolution of Sb-rich material then occurred, and filipstadite eventually crystallized in the cores. The presence around filipstadite of a zone depleted in Sb (Fig. 7), which coincides with the parts exhibiting the lamellar breakdown texture, provides a strong indication of such a process.

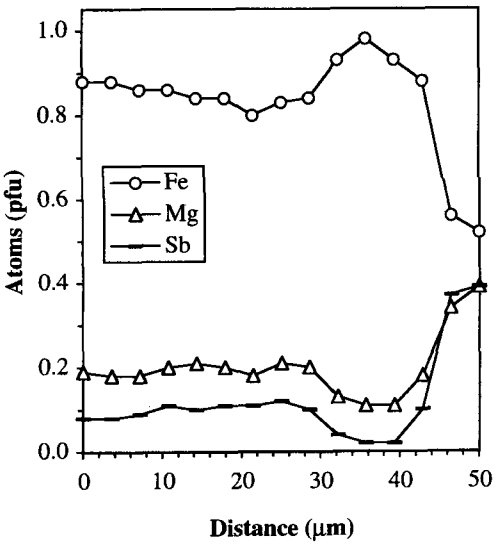

FIG. 7. Rim-to-core compositional profile for Fe, Mg and Sb from a spinel-type grain (iwakiite) in sample #KG2; the high Sb concentration in the core corresponds to filipstadite (cf. Table 5).

References

Björk, L. (1986) Beskrivning till Berggrundskartan Filipstad NV. *Sver. Geol. Undersök.*, **Af 147**, 1–110.

Boström, K., Rydell, H. and Joensuu, O. (1979) Långban — an exhalative sedimentary deposit? *Econ. Geol.*, **74**, 1002–11.

Brugger, J., Gieré, R., Graeser, S. and Meisser, N. (1997) The crystal chemistry of roméite. *Contrib. Mineral. Petrol.*, **127**, 136–46.

Dunn, P.J. (1986) Manganostibite: new chemical data, and its relation to kolicite and holdenite. *Geol. Fören. Stockholm Förhand.*, **109**, 101–2.

Dunn, P.J., Peacor, D.R., Criddle, A.J. and Stanley, C.J. (1988*a*) Filipstadite, a new Mn-Fe^{3+}-Sb derivative of

spinel, from Långban, Sweden. *Amer. Mineral.*, **73**, 413–9.

Dunn, P.J., Peacor, D.R., Criddle, A.J. and Stanley, C.J. (1988*b*) Ingersonite, a new calcium-manganese antimonate related to pyrochlore, from Långban, Sweden. *Amer. Mineral.*, **73**, 405–12.

Holtstam, D. (1993) A second occurrence of filipstadite in Värmland, Sweden. *Geol. Fören. Stockholm Förhand.*, **115**, 239–40.

Holtstam, D. (1994) Mineral chemistry and parageneses of magnetoplumbite from the Filipstad district, Sweden. *Eur. J. Mineral.*, **6**, 711–24.

Holtstam, D. and Langhof, J. (1995) Metamorphic harkerite from Nordmarks odalfält, Värmland, Sweden. *GFF*, **117**, 151–2.

Igelström, L.J. (1884) Manganostibiit, ett nytt mineral från Nordmarks grufvor i Vermland. *Öfversigt af Kongliga Vetenskaps-Akademiens Förhandlingar 1884*, **No 4**, 89–93.

Lundström, I. (1995) Beskrivning till berggrundskartorna Filipstad SO och NO. *Sveriges Geol. Undersök.*, **Af 177-185**, 1–218.

Magnusson, N.H. (1929) Nordmarks malmtrakt. *Sveriges Geol. Unders.*, **Ca 13**, 1–98. (Swedish with English summary)

Magnusson, N.H. (1930) Långbans malmtrakt. *Sveriges Geol. Unders.*, **Ca 23**, 1–111. (Swedish with English summary)

Mason, B. (1943) Mineralogical aspects of the system FeO-Fe_2O_3-MnO-Mn_2O_3. *Geol. Fören. Stockholm Förhand.*, **65**, 97–180.

Matsubara, S., Kato, A. and Nagashima, K. (1979) Iwakiite, $Mn^{2+}(Fe^{3+},Mn^{3+})_2O_4$, a new tetragonal spinelloid mineral from the Gozaisho mine, Fukushima prefecture, Japan. *Mineral. J.*, **9**, 383–91.

Moore, P.B. (1968) Contributions to Swedish mineralogy. II. Melanostibite and manganostibite, two unusual antimony minerals. The identity of ferrostibian with långbanite. *Ark. Min. Geol.*, **4(23)**, 449–58.

Moore, P.B. (1970*a*) Mineralogy and chemistry of Långban-type deposits in Bergslagen, Sweden. *Mineral. Record*, **1**, 154–72.

Moore, P.B. (1970*b*) Manganostibite: A novel cubic close-packed structure type. *Amer. Mineral.*, **55**, 1489–99.

Nysten, P. and Ericsson, T. (1994) Fe-rich långbanite from the Nyberget ore-field, Sweden. *Neues Jahrb. Mineral., Mh.*, 557–66.

Smith, D.C. and Perseil, E.-A. (1997) Sb-rich rutile in the manganese concentrations at St. Marcel-Praborna, Aosta Valley, Italy: petrography and crystal-chemistry. *Mineral. Mag.*, **61**, 655–69.

Pouchou, J.L. and Pichoir, F. (1984) A new model for quantitative X-ray microanalysis. I. Application to the analysis of homogeneous samples. *La Recherche Aérospatiale*, **3**, 13–36.

Raade, G., Mladeck, M.H., Din, V.K., Criddle, A.J. and Stanley, C.J. (1988) Blatterite, a new Sb-bearing Mn^{2+}-Mn^{3+} member of the pinakiolite group, from Nordmark, Sweden. *Neues Jahrb. Mineral., Mh.*, 121–36.

Shannon, R.D. (1976) Revised effective ionic radii and systematic studies of interatomic distances in halides and chalcogenides. *Acta Crystallogr.*, **A32**, 751–67.

Wink, B.W. (1996) Stability relations of antimony and arsenic compounds in the light of revised and extended Eh-pH diagrams. *Chem. Geol.*, **130**, 21–30.

[*Manuscript received 8 July 1997: revised 28 November 1997*]